Benchmarking of the new design tool InWave on a selection of wave energy converters from NumWEC project

Vincent Leroy, Adrien Combourieu, Maxime Philippe, Aurélien Babarit, François Rongère

BENCHMARKING OF THE NEW DESIGN TOOL *INWAVE* ON A SELECTION OF WAVE ENERGY CONVERTERS FROM *NUMWEC* PROJECT

Vincent Leroy[1], Adrien Combourieu[1], Maxime Philippe[1], Aurélien Babarit[2] and François Rongère[2]

[1]INNOSEA, Nantes, France

[2]LUNAM Université - Ecole Centrale de Nantes - CNRS, Nantes, France

Wave power has become an important field of research and development. Numerous wave energy converters (WEC) designs are being developed. Such systems efficiency needs to be evaluated and optimised to attract industrial investment. *InWave* is being developed to address this issue. This article presents an extended model to model comparison of *InWave* revisiting the *NumWEC* project, which gathers studies on 8 WECs inspired by existing devices. A full study has been conducted on 3 of these devices, including frequency domain results, motion and power RAOs and power matrices. Results show fair agreement and constitute a proof of concept of *InWave*.

Keywords: multibody systems, wave energy converter, numerical simulation

INTRODUCTION

WEC devices are complex to model with conventional seakeeping programs. Indeed, the articulations between bodies make the motion equation specific to each system and complex degrees of freedom (DoFs) appear.

To address this issue, flexible software is being developed. *InWave* [1] is based on a multibody dynamic solver which is able to build and solve directly the dynamic equation for a multibody tree structure. *InWave* also integrates a hydrodynamic potential solver.

The aim of this article is to verify *InWave* by modelling the same systems as in the *NumWEC* report [2]. In the *NumWEC* report, 8 different WECs were studied, expressing explicitly the motion equation for each of them.

In the first place, this article presents an overview of *InWave*. Then, it presents the comparison between *InWave* and the *NumWEC* report on three different devices. For each device, it compares frequency domain results, motion and power RAOs and power matrices.

PRESENTATION OF THE SOFTWARE

InWave [1] is a complete WEC modelling tool including incident wave generation, multibody dynamic solver, hydrodynamic solver, power take-off and mooring models, post-processing and visualization. *InWave* is based on a fast nonlinear semi-recursive dynamic solver inspired from robotics. It aims at modelling multibody offshore structures.

The multibody WEC is described as a number of bodies linked to each other's by articulations. The multibody structure is represented with a minimal set of degrees of freedom thanks to an efficient representation based on modified Denavit-Hartenberg parameterization as explained in [3].

InWave includes an equilibrium position research, an integrated and flexible BEM solver and a multibody dynamic solver. The multibody solver module works in time domain and is fully nonlinear. It solves the direct dynamic problem for a multibody structure. It means that it obtains its kinematics given the forces applied on the structure. Thanks to this approach, the set of equations to solve is minimal, both for the time domain and frequency domain solvers. The software's organization is shown in Figure 1.

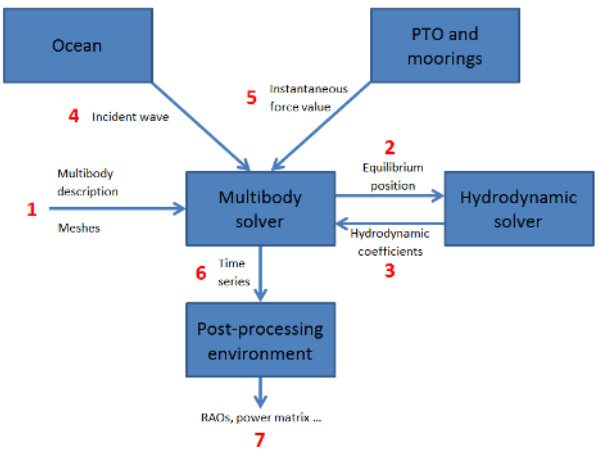

Figure 1: *InWave* architecture

The hydrodynamic loads are computed using time domain reconstruction from the hydrodynamic coefficient (excitation force, added mass and damping) computed in frequency domain under potential flow theory. The potential flow solver used is NEMOH, which is developed by Ecole Centrale de Nantes [4].

Simulations are run in time domain, for regular or irregular waves, leading to systems motions and power absorption. Results can be shown as times series, RAOs, spectral analysis, and power matrix.

MODEL TO MODEL VERIFICATION: PRESENTATION

InWave performances have been tested by comparison between *InWave* results and results from the *NumWEC* project [2] which was carried in 2011. It gathers studies on 8 different Wave Energy Converters (WEC). Power and motion RAOs and power matrices were calculated in this report. Frequency domain results were computed with the BEM code Aquaplus [5]. Each of the 8 devices has a different working principle. This paper focuses on 3 specific devices:

- A floating three-body oscillating flap device (F-3OF) inspired by *Langlee*
- A Bottom-standing Heaving Buoy Array (B-HBA) device inspired by *Wavestar*
- A bottom-standing oscillating flap device (B-OF) inspired by *Oyster2*

These systems do not intend to represent the commercial systems and were modelled for software verification only.

The main model differences between the models used in *InWave* and the ones used in *NumWEC* are explained in Table 1.

Table 1: Main differences between models

NumWEC	*InWave*
System specific motion equations are written	General multibody equations are used
$6 * n_{DOF}$radiation problems are solved by BEM	n_{DOF} radiation problems are solved by BEM
Linearized motion equation	Motion equation fully nonlinear
Linear hydrostatics	Nonlinear hydrostatics

VERIFICATION TEST CASE: *F-3OF* SYSTEM

Model

The *F-3OF* device is composed of a free underwater base and of four oscillating flaps. In [2], flaps are identified by pairs. The flaps are linked in rotation to the base (see Figure 2). Figure 3 shows a scheme of the *F-3OF* device as it is modelled in *InWave*. In mono-directional front waves, flaps located on the same side of the base have the same behaviour. The PTO systems are located at the links between the flaps and the base. They are supposed to act as linear dampers in the following.

Figure 2: *F-3OF* on *InWave* in irregular waves on *InWave*

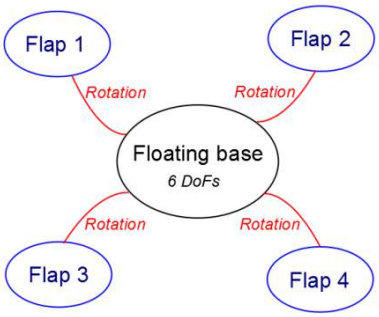

Figure 3: Multibody model of the *F-3OF* system in *InWave*

In this study, mono-directional waves propagating along x-axis are considered. Therefore, only surge, heave and pitch are highlighted in the following. Water depth is assumed to be infinite.

The forces applied on the system are listed below:

- Gravity
- Nonlinear hydrostatics
- Linear Froude-Krylov and diffraction force
- Linear radiation force
- Linear mooring along x-axis on the base body
- Linear power take-off on each flap hinge
- Morison drag is added on each body. Drag coefficient are taken from [2]

Nonlinear hydrostatics consists in integrating the static pressure over the instantaneous wetted surface. The Instantaneous wetted surface is obtained from the instantaneous body position and the instantaneous free surface elevation. The hydrostatic pressure is:

$$P(z) = -\rho * g * z$$

ρ being the volumetric mass of the sea water, g the gravity and z the position of a point on z axis. Nonlinear hydrostatics will differ from linear hydrostatics when the submerged volume of the body will encounter large variations. This is likely to happen either for large wave amplitudes, wave close to resonance or in the case of a body in rotation with a large lever arm (such as flaps).

The mesh used in this study is the same as the one used in [2], but some differences remain between the two models, as explained in Table 1.

Frequency domain results

The mesh used for hydrodynamic computations contains 1930 points and 1792 faces. The mesh convergence has been checked with a finer mesh. The mesh is presented in Figure 4. In practice, a mesh is provided for each body separately.

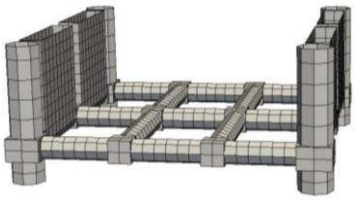

Figure 4: Mesh used for the F-3OF model

Frequency domain results from *InWave* have been compared with those from [2]. They show a very good agreement, as shows the example on Figure 5. Impulse responses are computed both for excitation force and radiation force (from damping coefficient only). They are further used in convolution integral to get the loads in time domain. They prove to be very similar between both models as well as shown on Figure 6. This validates the use of the BEM solver, which is completely integrated in *InWave*, and in which only relevant degrees of freedom are studied, instead of classical six degrees of freedom per body.

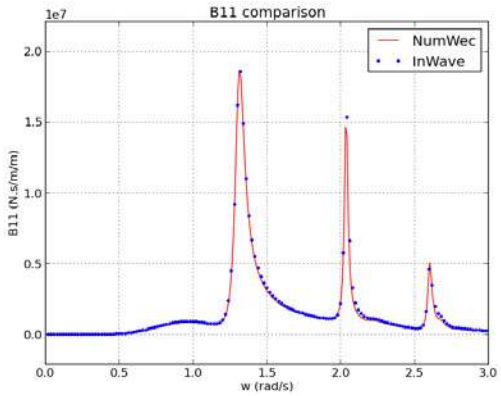

Figure 5: *F-3OF* Radiation damping (1,1)

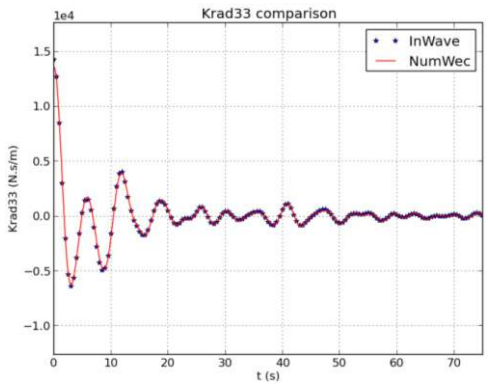

Figure 6: Krad (3,3) (radiation impulse response)

Regular waves simulations

Motion RAOs are constructed by harmonic analysis of the motion time series. Power RAOs are obtained taking the time average of the instantaneous extracted power.

In that case, simulations were run with constant wave amplitude (A=1m) with periods ranging in 5 – 15s. Simulations were run over 1000s with a time step of 0.1s. In order to avoid the transient effects, the first 400s were not taken into account in the post-processing. RAOs computed with *InWave* are compared with those from [2] computed in frequency and time domains.

Figure 7 shows the example of the pitch RAO of the base. Figure 8 shows the motion RAO of the first flap, Figure 9 shows the total power RAO of the device.

These RAOs show a fair agreement. The waves being 1m amplitude, the model's nonlinearities may have an influence and cause the differences, in particular at resonance.

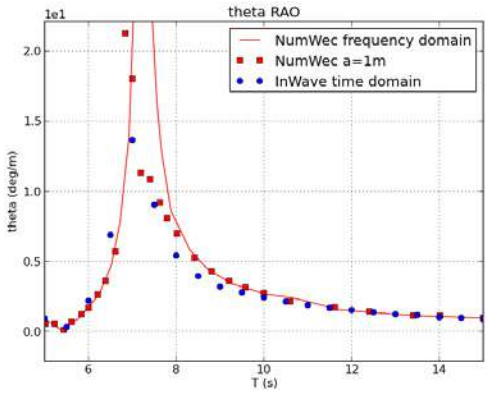

Figure 7: *F-3OF* Pitch RAO of the base

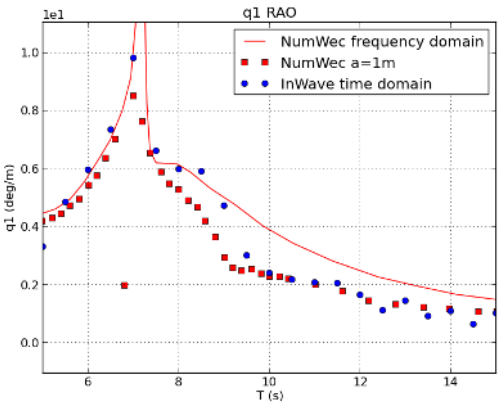

Figure 8: *F-3OF* Rotation RAO of the first flap

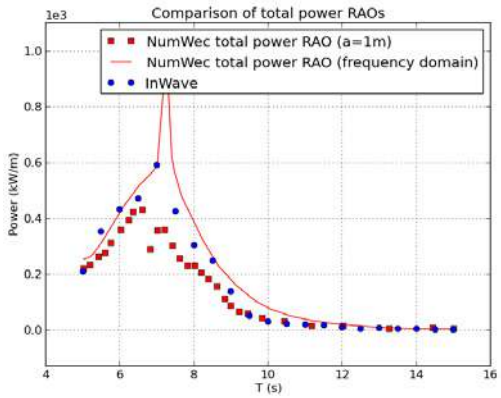

Figure 9: *F-3OF* total power RAO

Irregular wave simulations

Power matrices have been generated after simulations in irregular waves. Irregular waves are generated from a Jonswap spectrum with different values of significant height (H_s) and peak period (T_p). The "peakness" parameter γ is always taken to 3.3.Waves propagate in x direction and only.

Simulations are run over 1000s with a time step of 0.1s. In order to avoid transient effects, first 400s are discarded. A matrix is built gathering the mean values of extracted power, for a set of sea states (defined by H_s, T_p) likely to happen at Yeu site (France). The same matrix was built from *NumWEC* model with the same wave spectrums and PTO configuration. Both matrices are displayed in Figure 10 and Figure 11. Extracted power values in irregular waves obtained with *InWave* and *NumWEC* show quite good agreement. Trends are similar and maximums are located in the same place in the diagrams.

Differences were expected to grow with system motion, as *InWave* model introduces some nonlinearity that is not present in *NumWEC* model. Those nonlinearities come from several aspects of the model:

- Nonlinear hydrostatics is used
- The dynamic solver of *InWave* is fully nonlinear
- Morison drag on the flap is proportional to the square velocity of the body, which is obtained from nonlinear mechanics. Instantaneous values of this force are thus likely to be different in both models in case of large motion.

It can be observed in Figure 10 and Figure 11 that the bottom-right triangles of the power matrices (small steepness waves) match better than the top-left triangles. In fact, the top left cells correspond to large structure motion due to both large amplitude and wave periods close to resonance. With growing flap angles, the underwater profile of the structure is significantly changing. Taking into account nonlinear hydrostatics is thus expected to impact the results when large motions are happening.

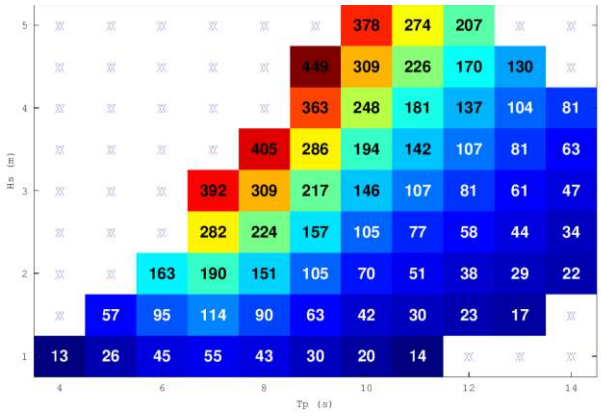

Figure 10: *F-3OF* power matrix obtained with *InWave*

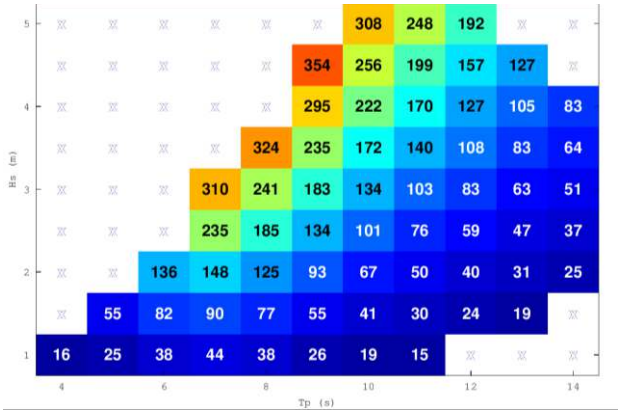

Figure 11: *F-3OF* power matrix obtained with *NumWEC*

VERIFICATION TEST CASE: *B-HBA*

Model

B-HBA is composed of a fixed base carried above the sea surface by four pillars and of 20 buoys fixed to the base. Figure 12 shows the geometry and the structure of the *B-HBA* device. This study focuses on a bottom-standing heaving buoy array device, a *Wavestar*-like system.

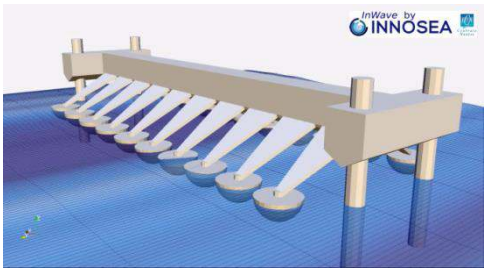

Figure 12: *B-HBA* device in irregular waves on *InWave*

The arm is 10m long, with an angle of 30° with the horizontal at equilibrium position. The buoys are 5m diameter. The platform is 70m long. There are many

interactions between buoys (diffraction and radiation), but this was not taken into account in [2]. In order to stay close from [2], only one single buoy was considered in this study to be consistent with NumWec model, but simulations with 20 buoys were also performed. The pillars were not taken into account in the hydrodynamic calculations. It has been established in [6] that the energy absorption is reduced by 20 % in a closely spaced array of heaving buoys. In the following, the buoy is considered to be the buoy and its arm. Figure 13 presents a scheme of the multibody model used in *InWave*.

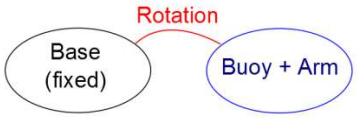

Figure 13: Multibody model of the *B-HBA* system in *InWave*

The differences between the two models remain the same as in Table 1.

The following forces are applied to the system:

- Gravity
- Nonlinear hydrostatics
- Linear excitation and diffraction force
- Linear radiation force
- Linear power take-off on the buoy rotation.

Frequency domain results

The mesh of the whole body and the mesh used for hydrodynamic calculations are presented in Figure 14. The mesh used for hydrodynamic calculation (excitation force, diffraction and radiation coefficients) contains 521 points and 400 polygons. The mesh convergence has been checked with a finer mesh.

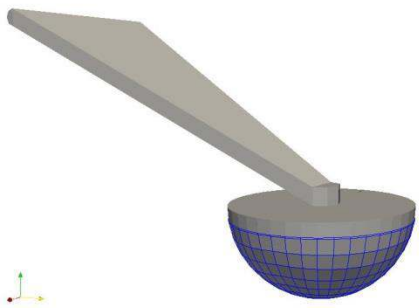

Figure 14: Mesh and hydrodynamic mesh of a *B-HBA* buoy

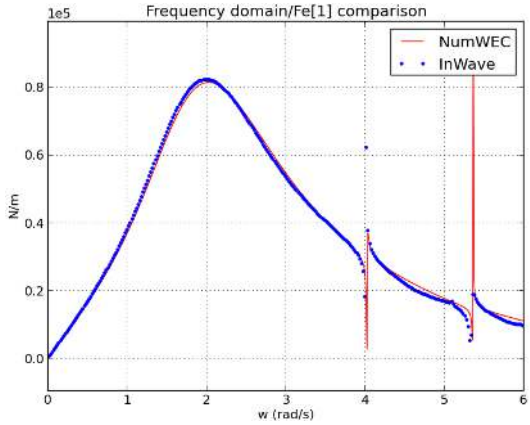

Figure 15: B-HBA - Fe(x) comparison

Frequency domain results of *InWave* have been compared with those from [2]. They show a very good agreement, as shown on Figure 15 with excitation force resultant on x axis. This validates the integration of the BEM solver in *InWave*, and the reduction of parameters to input into the BEM solver.

RAOs

RAOs were obtained after simulations in regular waves. In order to approach the linear model considered in the *NumWEC* report [2], small wave amplitudes were used (A=0.1m).

Motion and power RAOs have been calculated with different values of a PTO damping: Bpto = 2.5E6, 5E6, 7.5E6, 1E7, 1.5E7 N.m.s. These motion RAOs are plotted in Figure 16.

These RAOs show a good agreement for each PTO configuration. This shows that for small motions in small wave amplitudes, *InWave* stays close to linear theory.

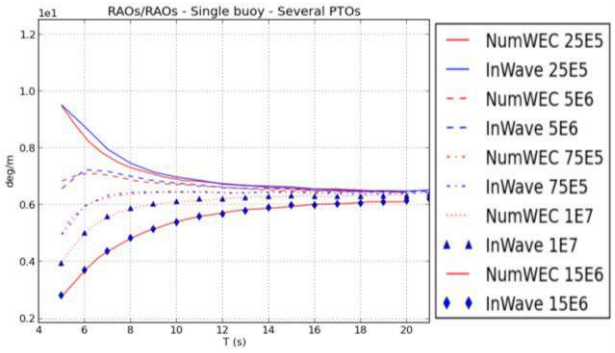

Figure 16: *B-HBA* – Motion RAO with several PTO settings

Irregular wave results

Power matrices have been generated after simulations in irregular waves. Irregular waves are generated from a Jonswap spectrum with different values of significant height (H_s) and peak period (T_p). The “peakness”

parameter γ is always taken to 3.3. Waves propagate in x direction.

Simulations are run on 1000s with a time step of 0.1s. In order to avoid transient effects, first 400s are discarded. A matrix is built gathering the mean values of extracted power, for a set of sea states (Hs, Tp). The same matrix has been built with the *NumWEC* model with the same wave spectrums and PTO configuration. Time domain simulations were performed with *NumWEC* model as well, but differences remain the same as in Table 1. *InWave* power matrix is plotted in Figure 17, *NumWEC* power matrix is plotted in Figure 18.

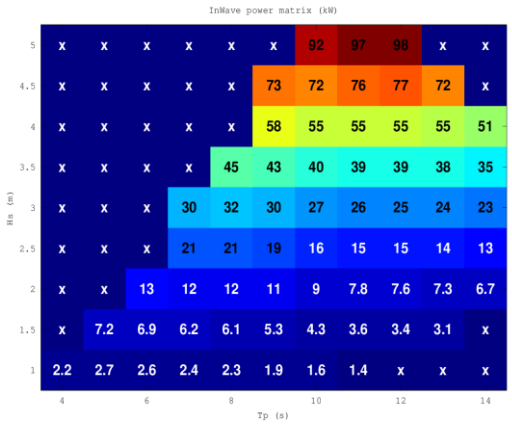

Figure 17: *B-HBA* power matrix from *InWave* irregular wave simulations

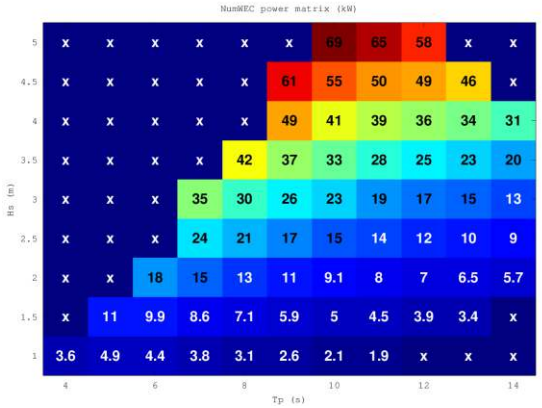

Figure 18: *B-HBA* power matrix calculated from the *NumWEC* model

InWave model is partly nonlinear. In particular, given the spherical shape of the B-HBA system, the nonlinear hydrostatics effect is expected to grow with body motion, inducing differences between the two numerical models. Nevertheless, similar trends between *InWave* and *NumWEC* models are observed in irregular waves.

.

VERIFICATION TEST CASE: *B-OF*

Model

B-OF is formed of a base fixed on the seabed, on which a flap rotates with the waves. It is a bottom-standing oscillating flap device inspired by the Osyter2 device shown on Figure 19. It is adapted for shallow waters (around 13m depth), the flap is water piercing. This study focuses on simplified *B-OF* geometry.

The power take-off system acts on the rotation of the flap. A scheme of the multibody model is presented in Figure 20.

In order to be the closest to *NumWEC* model, the following forces are applied to the flap:

- Linear excitation and diffraction force
- Linear radiation force
- Linear PTO on the flap's rotation
- In some cases, a spring term is implemented in the PTO
- Linear hydrostatic stiffness

The torque implemented at the hinge modelling the PTO forces is similar to a spring and damper:

$$\Gamma_{PTO} = -K_{PTO} * \theta_{flap} - B_{PTO} * \dot{\theta}_{flap}$$

Where:

- K_{PTO}: spring term of the PTO force
- θ_{flap}: angle of the flap from vertical
- B_{PTO}: linear damping term of the PTO force
- $\dot{\theta}_{flap}$: angular velocity of the flap

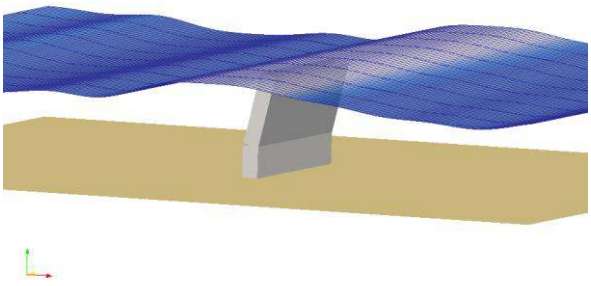

Figure 19: *B-OF* device in irregular waves on *InWave*

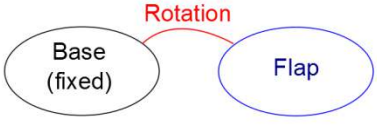

Figure 20: Multibody model of the B-OF system in InWave

Frequency domain results

The mesh used for hydrodynamic calculations contains 3460 points and 3228 faces, it is shown on Figure 21.

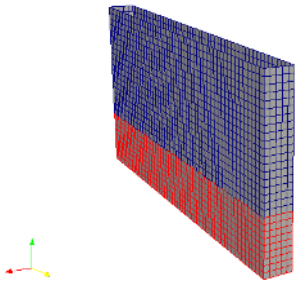

Figure 21: *Oyster* - meshes

Frequency domain results of *InWave* have been compared with those from the *NumWEC* report. They show a good agreement. For example, the comparison of the excitation torque on the rotation axis of the flap (θ) is plotted in Figure 22. This shows again the efficiency of the BEM solver which only focuses on relevant degrees of freedom. This is allowed by the use of relative coordinates between the bodies.

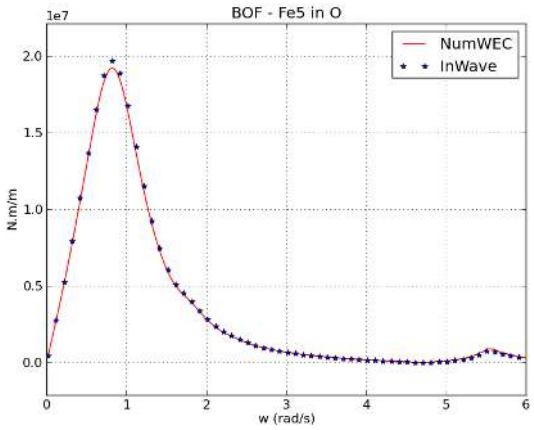

Figure 22: *Oyster* 2 - Comparison of excitation force torque on rotation of the flap

Regular wave results

RAOs were obtained after time domain simulations in regular waves. In order to approach the linear mechanics model considered in *NumWEC* report [2], small wave amplitudes were used ($A = 0.1m$).

Motion and power RAOs have been calculated with $B_{PTO} = 1.0E7\frac{N.m}{rad.s^{-1}}$ and $K_{PTO} = 0\ N.m/rad$ and compared with those from the *NumWEC* report. These RAOs show a good agreement, which highlights the fact that *InWave* stays close to linear theory for small motions in small wave amplitudes. The motion and power RAOs are plotted in Figure 23 and Figure 24.

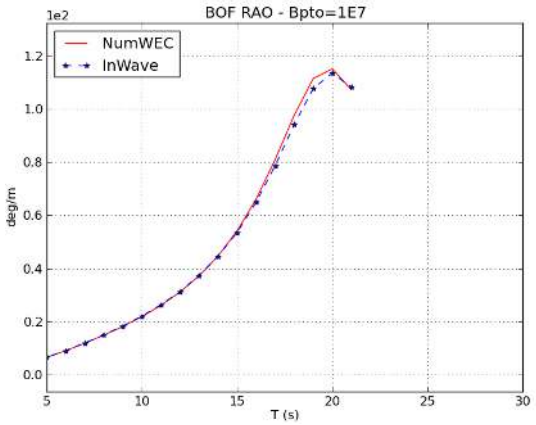

Figure 23: *B-OF* – Comparison of motion RAOs

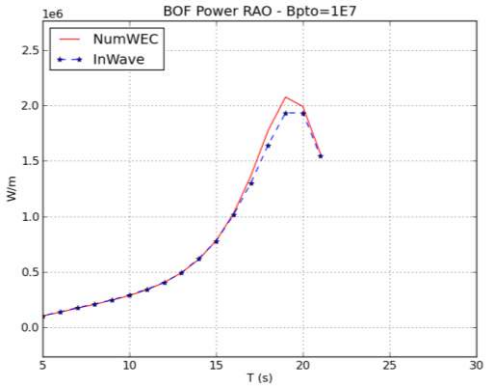

Figure 24: *B-OF* - Comparison of power RAOs

Irregular wave results

Simulations have been performed in irregular waves with *B-OF*.

Optimised PTO parameters were used for B_{PTO} and $K_{PTO}$for each sea state. Morison type viscous damping has been implemented for each vertical section of the flap according to the following formula:

$$\overrightarrow{F_{v,i}(M_i)} = -\frac{1}{2} * \rho_{water} * C_v * A_i * \left(\overrightarrow{V(M_i)} - \overrightarrow{V_{water,0}(M_i)}\right) * \left\|\overrightarrow{V(M_i)} - \overrightarrow{V_{water,0}(M_i)}\right\|$$

Where:

- M_i is middle point of section i
- C_v is the drag coefficient
- A_i is the cross section area of section i
- $\overrightarrow{V(M_i)}$ is the velocity of the centre of section i
- $\overrightarrow{V_{water,0}(M_i)}$ is the water velocity of the undisturbed incident wave

Hydrodynamics nonlinearities appear in the model from this implementation of the viscous damping.

A power matrix has not been built but Table 2 presents the results of some irregular wave simulations. The results show a fair agreement but some differences appear.

These differences between the models in irregular waves with Morison drag implementation are assumed to come partly from the impact of Morison drag through nonlinear dynamics of *InWave*: as Morison drag depends on the velocity of the body, it is dependent on the dynamics model. Differences may also come from the irregular wave random generation. Irregular wave time series are generated from Jonswap spectrum. Random phases are not the same in both models resulting in different wave elevation time series. This can slightly affect the time averages.

Sea state		Mean power (W)		Relative error
T_P (s)	H_S (m)	*InWave*	NumWEC	(%)
8	5	2,02E+06	1,96E+06	3%
7	3,5	8,76E+05	9,34E+05	6%
3	1	1,71E+04	1,57E+04	9%
10	2	3,44E+05	3,83E+05	10%
5	1,5	8,24E+04	9,22E+04	11%
12	2,5	4,42E+05	5,19E+05	15%
6	2,5	3,17E+05	3,78E+05	16%
10	4	1,18E+06	1,43E+06	18%

Table 2: BOF - Irregular wave simulations results

CONCLUSION

In this paper, the generic multibody solver *InWave* was verified on three test cases against system specific programs.

Hydrodynamic coefficients (added mass, damping and excitation force) are showing perfect agreement which validates the coupling between mechanic and hydrodynamic solvers.

InWave time domain simulations in small waves are matching with frequency domain simulations from *NumWEC*, giving confidence in the time domain reconstruction and the dynamic solver. Indeed, in small wave amplitudes, *InWave* agrees with linear theory results.

Finally, time domain simulations in irregular waves show fair agreement between the two time domain models. Differences appear where expected, because of some nonlinearities present in *InWave* model.

Proof of concept is therefore reached. Further validation of *InWave* against experimental data is currently undergoing.

REFERENCES

[1] A. Combourieu, M. Philippe, F. Rongère et A. Babarit., "InWave: a new flexible design tool dedicated to wave energy converters", OMAE2014-24564.

[2] A. Babarit, J. Hals, A. Kurniawan, M. Muliawan, T. Moan et J. Krokstad, "The NumWEC project - Numerical estimation of energy delivery from a selection of wave energy converters", 2011.

[3] F. Rongère et A. Clément, "Systematic Dynamic Modeling and Simulation of Multibody Offshore Structures: Application to Wave Energy Converters", OMAE2013-11370.

[4] LHEEA. [En ligne]. Available: http://lheea.ec-nantes.fr/doku.php/emo/nemoh/start.

[5] G. Delhommeau, "Seakeeping codes Aquadyn and Aquaplus", In Proc. Of the 19th WEGEMT school, numerical simulation of hydrodynamics: ships and offshore structures, 1993.

[6] G. De Backer, M. Vantorre, C. Beels, J. De Rouck et P. Frigaard, «Power absorption by closely spaced point absorbers in constrained conditions,» *IET Renewable Power Generation,* vol. 4(6), pp. 579-591, 2010.